Research on Force Interaction Devices Specialized for Blind Guidance Robot

Bin Hong[1,2,3], Meimei Chen[1,2], Yihang Guo[1,2], Fugeng Li[1,2], Changyuan Feng[1,2], Zhan Cao[1,2], Zhihao Ma[1,2] and Jing Hou[1,2,3,*]

[1]*Vehicle Intelligence and Simulation Engineering Laboratory, Internal Combustion Engine Research Institute, Tianjin University, Tianjin, China*

[2]*School of Mechanical Engineering, Tianjin University, Tianjin, China*

[3]*Tianjin Tianbo Science & Technology Co., Ltd., Tianjin, China*

Abstract: As a new type of human-computer interaction, physical human-robot interaction is very common in guide robots and is the mainstream of future development. However, the force interaction device is hard to choose according to actual application requirements. In this paper, we compared the force transmission characteristics of three interaction mediums: rigid rod, spring-damping, and cable. The result shows that the rigid rod will bring a force impact on blind users when the robot's motion state switches, while the spring-damper can not perform well in its response and stability. In contrast, the cable is more suitable in this area for its fast response and stability, moreover, it does not impose a dramatic impact when imposing an excitation force.

Keywords: Guide robots, Josso interaction, Human-robot interaction, Smart devices.

1. INTRODUCTION

In recent years, as automation and intelligent technology develops rapidly, blind guidance robots have emerged as an alternative to guide dogs to provide walking guidance for blind people. Currently, the major structural modes of blind guidance robots include small electronic guide devices, guide canes, wearable guide devices, and mobile guide devices. Regardless of the mode, an effective guidance process should be based on the good interaction effect.

Nowadays, common interaction methods for blind guidance robots include auditory-based interaction [1, 2], tactile-based interaction [3-9], and force-based interaction [10-12]. Compared with auditory-based interaction, tactile and force-based interaction are insufficient to the richness of interaction information, but they can compensate for the instability and susceptibility to the interference of voice interaction and deliver key guidance instructions in a timely and effective manner. Compared to traditional tactile interaction devices, including vibration motors and Braille display, force interaction can reduce the burden of understanding specific sequences for blind people and make the interaction process more efficient. For mobile blind guidance robots, convenient interaction during guidance is especially important because they are equipped with independent power units, and force-based interaction has attracted enough attention due to its naturalness and simplicity, which has opened up a new research direction - physical human-robot interaction (pHRI).

Address correspondence to this article at Vehicle Intelligence and Simulation Engineering Laboratory, Internal Combustion Engine Research Institute, Tianjin University, Tianjin, China; E-mail: houjing1102@163.com

A common interaction medium for force-aware blind guidance robots is the rigid rod. Gerard *et al*. [13] proposed a guide robot called PAM-AID, in which the user input device is a joystick with a switch mounted on an armrest. The University of Michigan's Mobile Robotics Lab has developed a Guide-Cane, a class of mobile blind guidance robots in which a blind person can use a thumbstick to prescribe a desired direction of motion and to perceive changes in the robot's state of motion. Dae *et al*. [12] also used a joystick as the interaction medium to develop a user-steered blind guidance robot that applies a fuzzy logic controller to recognize the user's intention and adjust its linear and angular velocity. Recently, Dr. Lee *et al*. at Berkeley [14] used a leash as an HRI medium to study the switch between taut and slack states for obstacle avoidance, they also proposed a hybrid pHRI model involving tension to describe the dynamics of the robot guidance system. Similarly, in the field of UAVs, Marco *et al*. [15] used the tether as an interaction medium to achieve a robot capable of only using force as an indirect communication channel to bring a human to the desired location (or along a path).

As shown in Dae's research [12], when blind users walk fast or turn sharply, they will feel obvious discomfort in their hands and shoulders by the joystick. Even though the problem could be solved by proposing an optimization algorithm, it would be more effective to consider it when selecting the interaction device. A point worth considering is that the switch in the motion state of the blind guidance robot shows different characteristics for the blind person's hand end when different interaction devices are applied. The purpose of this paper is to investigate the force transmission effect on when the rigid rod, springs, and flexible cable are used as interaction devices, to select the optimal

E-ISSN: 2409-9694/23 © 2023 Zeal Press

medium of interaction, and determine the relevant parameters according to the proposed criteria.

Section 2 focuses on modeling the mechanics of the three force interaction mediums. Section III carries out simulation analysis based on ADAMS for the relevant models. Section IV carries out experimental validation on the existing prototype platform. Section V summarizes the research content of this paper, as well as proposes further research plans for the current deficiencies.

2. MODEL ESTABLISHMENT

2.1. Force Transmission Model of the Rigid Rod

When a blind person is interacting with the blind guidance robot using a rigid rod as the medium, at this time the robot needs to accelerate due to some special requirements, such as obstacle avoidance. Assume that its traction force changes abruptly from one constant force to another constant force within a certain period, and we set it as a step force.

For the blind person, he starts to adjust his speed after receiving the sudden impact in force. In other words, the hand end of the blind person can be regarded as the hinge structure connected with the rigid rod in a short period. Therefore, the period at the moment of the sudden step force can be approximated as equilibrium and analyzed from the point of static equilibrium.

The equilibrium state where the pull force is imposed is depicted in Figure **1**, and $\overrightarrow{F_i}$ (i=1,2,3) are the forces contained in this model, where $\overrightarrow{F_3}$ (value=F) is the horizontal pull force imposed by the blind guidance robot, $\overrightarrow{F_2}$ (value=mg) is the self-gravity of the rigid rod, and $\overrightarrow{F_1}$ (value=T) is react force on the hand end of the blind person transmitted by $\overrightarrow{F_3}$. According to the theorem of concurrence of three balanced forces, the extension line of the force vector $\overrightarrow{F_1}$, $\overrightarrow{F_2}$ and $\overrightarrow{F_3}$ will intersect at a point, indicated as the point O. The included angle of the negative direction of the x-axis and $\overrightarrow{F_1}$ is recorded as θ.

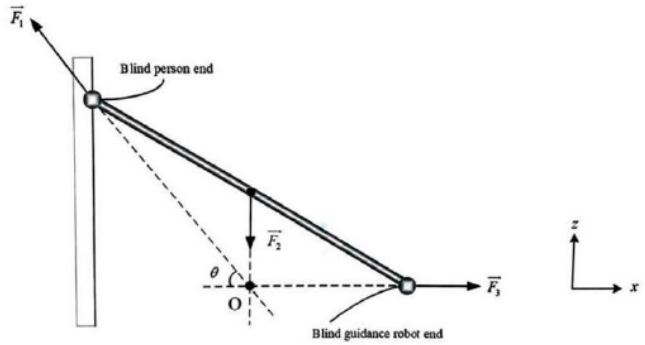

Figure 1: The model description when a step force is imposed on the rigid rod.

Four static equilibrium equations of (1) – (4) can be obtained according to the force on the rigid rod force transmission model in Figure **1**.

$$\sum_{i=1}^{3} \overrightarrow{F_i} = 0 \tag{1}$$

$$\left\|\overrightarrow{F_1}\right\|, \left\|\overrightarrow{F_2}\right\|, \left\|\overrightarrow{F_3}\right\| = F, mg, T \tag{2}$$

$$\overrightarrow{F_2} = -Proj_z\left(\overrightarrow{F_1}\right),\ \overrightarrow{F_3} = -Proj_x\left(\overrightarrow{F_1}\right) \tag{3}$$

$$\left\|\overrightarrow{F_1}\right\|^2 = \left\|\overrightarrow{F_2}\right\|^2 + \left\|\overrightarrow{F_3}\right\|^2 \tag{4}$$

The above equation shows that the reacting force $\overrightarrow{F_1}$ is tightly related to the force vector $\overrightarrow{F_2}$ and $\overrightarrow{F_3}$. If the value of $\overrightarrow{F_2}$ is small enough compared to that of $\overrightarrow{F_3}$, θ will decrease to 0, and the value of $\overrightarrow{F_1}$ will keep in sync with that of $\overrightarrow{F_3}$ in the opposite direction.

2.2. Force Transmission Model of the Spring-Damping

Typically, when in the application of using cable as the pHRI medium, the model of the force is typically calculated by Hooke's law. According to Tognon's description [4], that is, when the cable is slack, the cable force intensity is zero and when the cable is taut, the cable force intensity is proportional to the increment of the cable length. It can satisfy the following equation:

$$t_c\left\|\overrightarrow{l_c}\right\| = \begin{cases} k_c\left(\left\|\overrightarrow{l_c}\right\| - \overline{l_c}\right) \ if\ \left\|\overrightarrow{l_c}\right\| - \overline{l_c} > 0 \\ 0\ otherwise \end{cases} \tag{5}$$

Where $\overline{l_c}$ is the constant nominal length of the cable, $\overrightarrow{l_c}$ is the vector from the blind guidance robot end to the blind person's end, k_c is the constant elastic factor, $t_c\left\|\overrightarrow{l_c}\right\|$ represents the cable internal force intensity.

Actually, it also exists damping force in the dynamic motion of the cable, which is proportional to the cable motion velocity. In this case, we take the damping factor into the existing spring model for consideration and explore the tension in the spring-damping interaction system when imposed a step force.

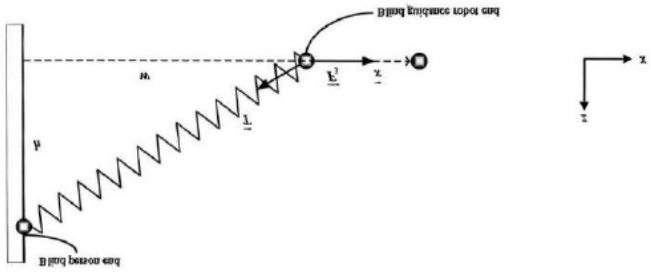

Figure 2: Example of a translational spring-damper model.

The magnitude of the translational force of a spring-damper is linearly dependent upon the relative displacement and velocity of the two locations that define the endpoints of the spring damper. Replacing

the rigid rod with a spring-damping element also derives a law for the variation of the spring force with the motion state of the blind guidance robot (shown in Figure **2**), *i.e*.

$$\left\|\vec{T}\right\| = C \cdot (d\|\vec{r}\| / dt) + K \cdot (\|\vec{r}\| - L) + \left\|\overrightarrow{F_{pre}}\right\| \quad (6)$$

where $\vec{r}$ refers to the distance between the two relative coordinate points that define the spring-damping, $d\|\vec{r}\| / dt$ refers to the relative velocity of the two coordinate points, C refers to the damping factor, K refers to the spring stiffness factor, $preload$ refers to the reference force of the spring, and L refers to the reference length, and the value of $force$ is $\left\|\overrightarrow{F_{pre}}\right\|$ when $r = L$.

According to the geometric relationship, it can obtain that:

$$\vec{r} - \vec{L} = \vec{x} \quad (7)$$

$$\|\vec{r}\|^2 = h^2 + (w + \|\vec{x}\|)^2 \quad (8)$$

Then the end motion of the blind guidance robot is analyzed by Newton's second law,

$$\left\|\overrightarrow{F_3}\right\| - \left\|\vec{T}\right\| \cdot cos\varphi = m_0\|\ddot{\vec{x}}\| \quad (9)$$

where m_0 is the mass of the blind guidance end, φ refers to the angle where vector $\vec{r}$ intersects with the negative direction of the x-axis, which can be expressed as:

$$cos\varphi = \frac{w+\|\vec{x}\|}{L} \quad (10)$$

Joint equations (6), (8) and (9), the relationship between the spring force $\left\|\vec{T}\right\|$ and imposed pull force $\left\|\overrightarrow{F_3}\right\|$ would be derived in theory.

2.3. Force Transmission Model of the Flexible Cable

According to the previous survey, studies applying flexible cable as pHRI medium are quite rare, while the mass of flexible cable tends to be neglected and its elasticity is the focus. Here, the cable catenary model is used to describe the dynamic characteristics of the flexible cable. Although the lumped mass method shows more advantages in describing the dynamic response of cable, its application scenario is generally deep-sea mooring and towing where the mass of cable is quite large. Moreover, it needs sufficient moving boundary conditions and initial conditions to solve it, while the blind person's motion state is uncertain in pHRI interaction.

The mass of the flexible cable itself selected for interaction will not be too heavy, so the inertia force caused by acceleration can be appropriately ignored in the case of the flexible cable in the shape of the catenary. The static analysis of the flexible cable is carried out by the s catenary equation to solve for the tension at the end of the flexible cable.

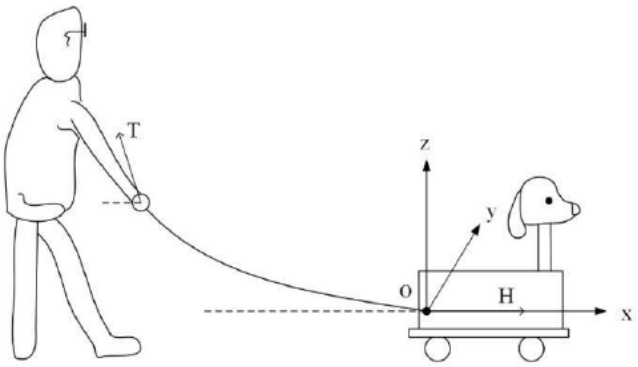

Figure 3: Depiction of a flexible cable model.

As shown in Figure **3**, the origin of the three-dimensional coordinate system is established at the end of the flexible cable connected to the blind guidance robot. For ease of calculation, when the total system is in a dynamic process, the origin of the coordinate system will move with the motion of the robot, forming a dynamic coordinate system. From this, the configuration equation of the flexible cable when it is not straightened can be expressed by the catenary equation as:

$$z(x) = -\frac{H}{\rho g} + \frac{H}{\rho g} cosh(\frac{\rho g}{H} x) \quad (11)$$

where ρ is the line density of the cable, H is the horizontal tension imposed on the robot end.

Set the blind person's end of the horizontal distance from the end of the robot to x_port, flexible cable length is a constant value of L, derived from equation (12), then the horizontal tension H can be solved by equation (13):

$$\int_{-x\_port}^{0} \sqrt{1 + z'(x)^2}\, dx = L \quad (12)$$

$$\frac{H}{\rho g} sinh\frac{\rho g}{H} \cdot x\_port = L \quad (13)$$

Similarly, when the horizontal tension H is given, its corresponding x_port can also be calculated, then the shape curve of the flexible cable will be depicted. Moreover, the gravity and the force imposed on the hand end can be derived from the following equations:

$$G(\mathrm{x}) = \rho g L(x) = H\, sinh\frac{\rho g}{H} x \quad (14)$$

$$T(x) = \sqrt{H^2 + G^2(x)} = H\, cosh\frac{\rho g}{H} x \quad (15)$$

When the selected cable could be stretched due to its elasticity, the influence of the elastic modulus on the results cannot be ignored when solving with a catenary

equation, and the elastic modulus is introduced into the classical suspension line equation for correction, resulting in the elastic suspension line equation.

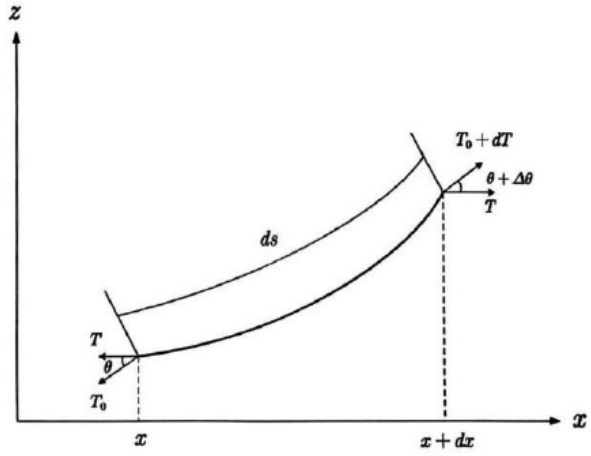

Figure 4: Force on a micro-segment of the catenary segment.

As shown in Figure **4**, the flexible cable micro-element segment ds is selected for the study. Its mechanical equilibrium equation is:

$$\begin{cases} (T_0+dT)\cos(\theta+\Delta\theta)=T_0cos\theta=T \\ (T_0+dT)\sin(\theta+\Delta\theta)=T_0sin\theta+\rho gds \end{cases} \quad (16)$$

The above equation can be divided to obtain:

$$\tan(\theta+\Delta\theta)-tan\theta=\frac{\rho g}{\mathrm{T}}ds \quad (17)$$

Taking the limit to derive:

$$tan'\theta\frac{d\theta}{dx}=\frac{\rho g}{T}ds \quad (18)$$

According to $z''=tan'\theta\frac{d\theta}{dx}$,

$$z''=\frac{\rho g}{T}ds=\frac{\rho g}{T}\sqrt{1+(\frac{dz}{dx})^2}dx \quad (19)$$

By Hooke's law and the conservation of mass, the mass of the flexible cable before and after the force deformation is constant, then we have

$$\rho_0=\frac{\rho}{1+\frac{T_0}{EA}} \quad (20)$$

Set $\varepsilon=\frac{T}{EA}$, take $a=\frac{\rho_0 g}{T}$, $\frac{dz}{dx}=sinhu$ into the equation (19) and (20), it can be expressed as:

$$coshudu=\frac{acoshu}{1+\varepsilon coshu}du \quad (21)$$

dx is expressed by du, and the integral of u is obtained

$$x=\frac{1}{a}(u+\varepsilon sinhu)+C_1 \quad (22)$$

Similarly, it can be obtained that

$$y=\frac{1}{a}\left(coshu+\frac{1}{2}\varepsilon cosh^2h\right)+C_2 \quad (23)$$

3. SIMULATION RESULTS

The force transmission simulation of rigid rod and spring-damper was conducted on Adams software. As shown in Figure **5**, a rigid rod and spring-damping were set as the interaction medium between the blind person and the blind guidance robot. According to the actual situation, the horizontal and vertical distance of the connection points at the two ends were set to 0.98m and 0.88m, respectively. Meanwhile, the diameter of both the rigid rod and the spring-damping is set to 0.03m and 0.08m, respectively. The mass of the rigid rod is set to 0.1kg, while the mass of the spring damping is negligible in the software.

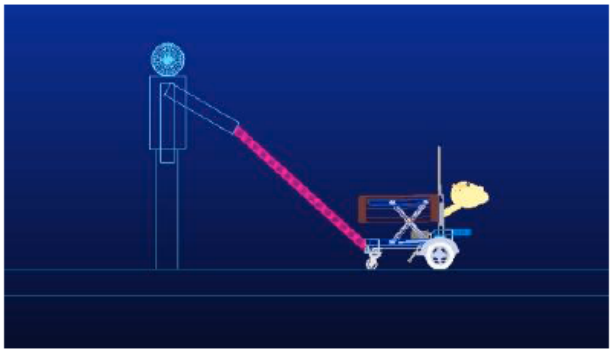

Figure 5: (a) Simulation model diagram under rigid rod interaction medium.

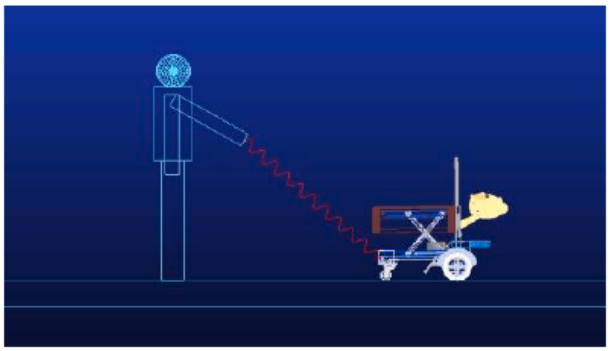

Figure 5: (b) Simulation model diagram in spring-damped interacting media.

This simulation provides a preliminary study of the force transfer effect of the rigid rod and spring-damping where the stiffness factor and damping factor were set to 5 newton/meter and 1 newton-sec/meter respectively.

To better illustrate this phenomenon, we set the upper boundary of the step force to 7N, 12N, 17N, 22N, 27N, and 32N respectively, shown in Figure **4**. It can be seen that when the rigid rod is selected, the force transmitted to the hand end also changes sharply when the exaction force imposes. The force transmission is without any depletion. In contrast, when the

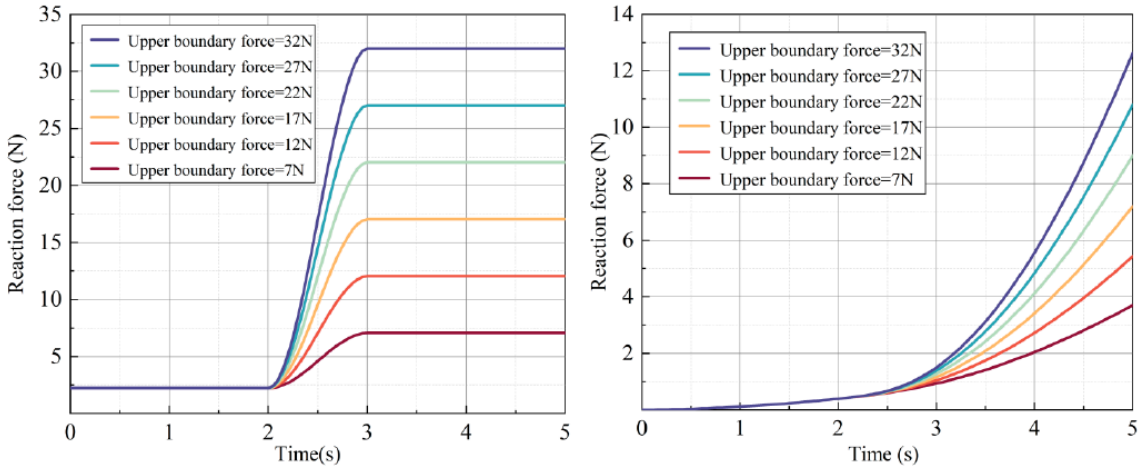

Figure 6: The force transmission effect when the interaction medium is a rigid rod(left) and is spring damping(right).

spring-damping is used as the interaction medium, the force that reacts on the hand end increases slowly during the 2-3s period, whether the step force increases to 7N or 32N. This initially shows that spring-damping can reduce the pulling force impact of the blind guidance robot due to motion state switch to some exten.

It can be seen that the rigid rod can effectively transmit the tension force, but it also causes an apparent impact on the blind person when switching between motion states, while the spring has a certain delay effect on the force transmission.

To investigate the effect of spring-damping physical parameters on the delay effect of tension, the tension input of the blind guidance robot was set to STEP (Time,2,2,3,7), and the stiffness and damping factors were changed to observe the effect of the imposed force. As shown in Figure **7**(left), when the stiffness factor of the spring keeps increasing, the force response at the blind hand end becomes faster accordingly.

For different damping factors, it does not have a good effect on improving the transmission effect of excitation force by adjusting its values. As shown in Figure **7**(right), theoretically, the force transmission is gradually improved by increasing the value of the damping factor. However, in the actual value of the damping coefficient, the magnitude of change in the damping coefficient is very small, and the effect of changing the damping coefficient on the improvement of the spring force transmission hysteresis is negligible.

In addition to the case of abrupt changes in tension, another case is that of a blind guidance robot pulling a blind person along with a constant force under ideal conditions, and simulations were performed in this case. It is found that when one end is loaded with a constant force, the spring-damped force transfer has a fluctuation, which decreases in response to increasing its damping coefficient, while it is difficult to suppress this fluctuation when changing the stiffness coefficient (Figure **8**).

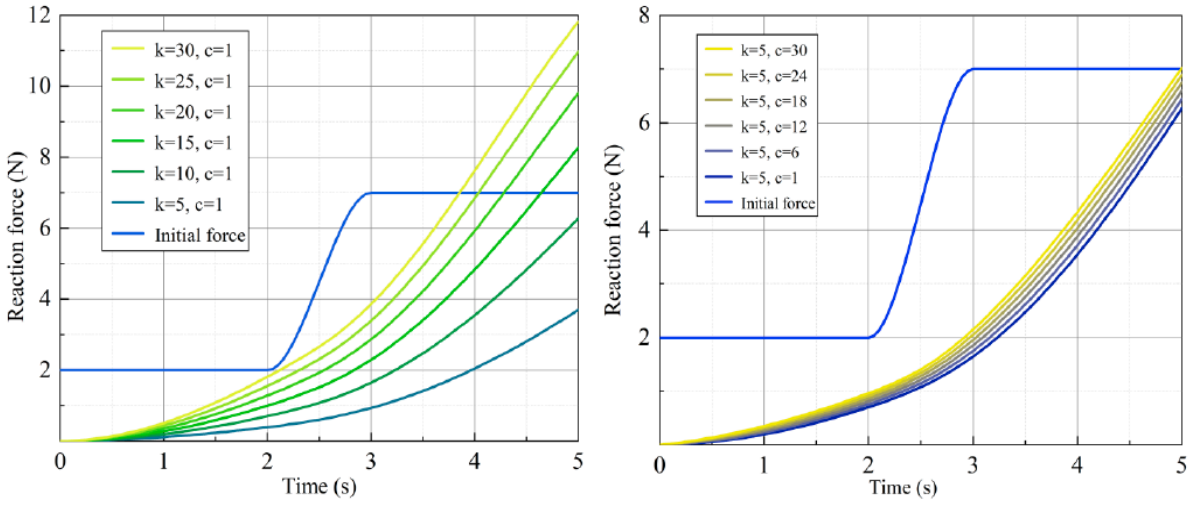

Figure 7: The force transmission effect when applying different stiffness factors (left) and damping factors (right).

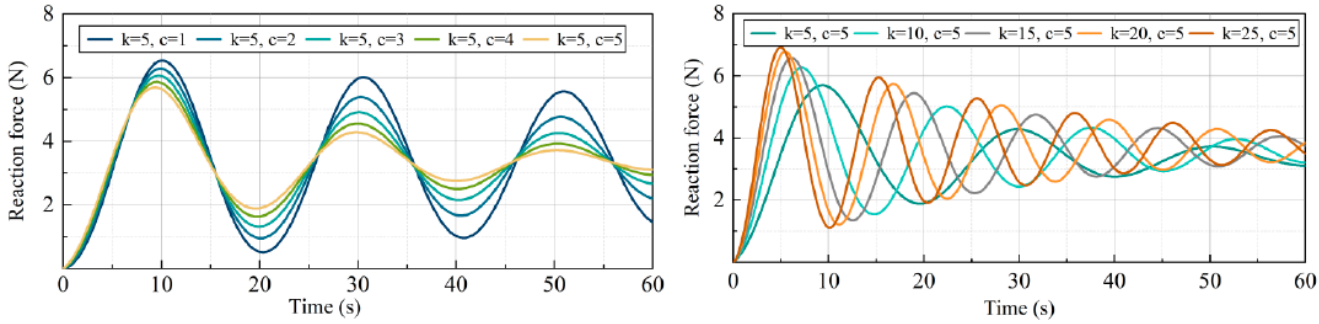

Figure 8: The force fluctuation effect when applying different damping factors (left) and stiffness factors (right).

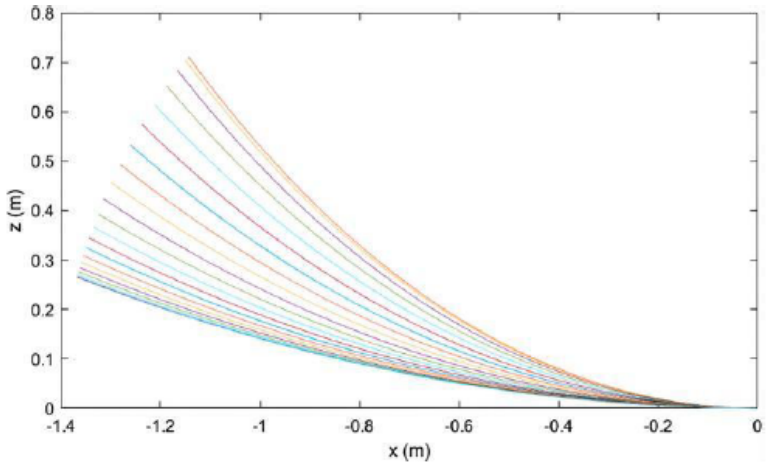

Figure 9: Catenary configuration corresponding to a step force at one end.

It can be seen that the selection of a spring-damping to meet the human-robot interaction requires a balance between the need for fast force response and low fluctuation. To some extent, although increasing the stiffness coefficient can suppress the problem of slow spring force transfer response, the damping coefficient is small, which makes it difficult to meet the need for reducing volatility. Therefore, spring-damping may not be the best choice as a human-robot interaction device for blind guidance robots.

To facilitate the calculation, we set the blind guidance robot end as the coordinate origin and study the force fluctuation applied to the blind hand end when a step force of the same 2-7N is applied to the pulling force at the guide robot end. Based on the step force discrete point, the coordinates of x_port at each moment are calculated according to equ (13), and then the magnitude of the corresponding top pull at each moment is obtained according to the formula for the pull force T.

The Catenary configuration when a step force at one end is depicted in Figure **9**, as the force intensity increases, its corresponding configuration will slow down.

4. EXPERIMENTAL RESULTS

This summary focuses on the rigid rod, the spring and the flexible cable as the guiding media connecting the subject to the guide robot. The three mediums are given a horizontal sudden change in pulling force at the end of each medium. This means that at a given moment the robot applies a step pull to the end of the guide medium. The data is then collected in real time by a tension sensor at the end of the guide robot. Finally, a set of step pull response curves for each of the three media was obtained, and the relevant theory and simulations mentioned in this paper were experimentally verified, as shown in Figure **10**.

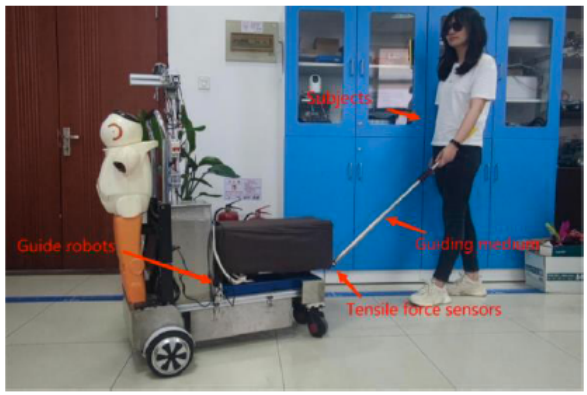

Figure 10: Schematic diagram of the experimental procedure.

Table 1: Basic Parameters of the GDR

Basic Parameters	Numerical Values
Overall mass m (kg)	120
Full load mass M (kg)	150
Wheel rolling radius r (mm)	100
Air resistance coefficient C_D	0.96
Rolling resistance factor f_r	Generally set to 0.01
Windward area A (m^2)	0.4
Rotating mass conversion factor δ	1.04
System mechanical efficiency η_T	0.9

Based on the initial set of power performance indicators for the guide dog robot, preliminary calculations of the power parameters of its drive system are carried out to derive the peak power, torque and speed requirements for the guide dog robot under various operating conditions, which serve as an important basis for motor selection. The basic parameters of the guide dog robot are shown in Table **1**.

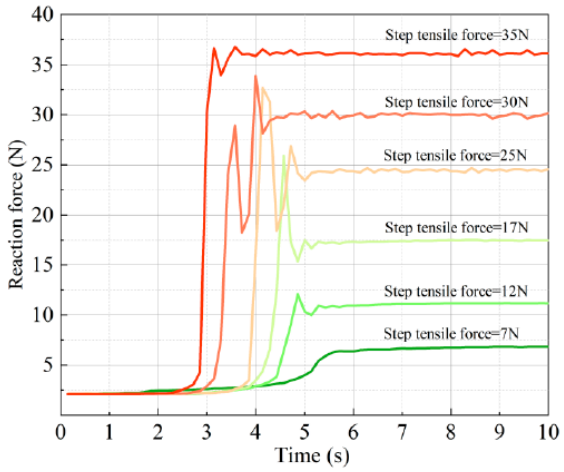

Figure 11: Rigid rod force perception interaction tension step response curve.

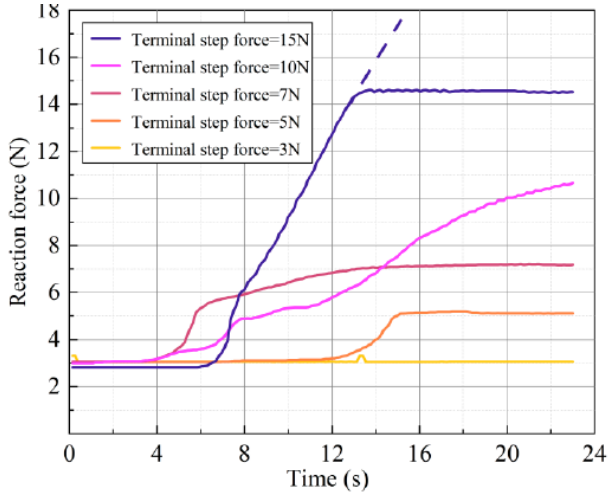

Figure 12: Spring force sensory interaction tension step response curve.

The pull response curve for the rigid rod guide is shown in Figure **11**. The horizontal coordinates represent time and the vertical coordinates represent the tension values. The horizontal sudden change in pull force at the end of a rigid rod is given. That is, the guide robot applies a step pull of 5N-35N to the end of the rigid rod over a period of 2-6s. The horizontal tension applied to the end of the rigid rod is shown in the colour curve in Figure **11**. The tension applied to the first end of the rigid rod can be expressed as a composite of the gravitational force of the rigid rod and the horizontal tension at the end. Data was collected using a tension sensor at the end of the guide robot and the force curve was plotted on an Origin software post-processor.

Due to the gravity of the rigid rod and the limitations of the experimental conditions, the force curve fluctuates around the peak and has an initial value of approximately 2.5 N. The experimental data curve in Figure **11** shows that the rigid rod conducts the force very rapidly, with a rise time of almost less than 0.1 s when the applied force F > 10 N. This results in a large acceleration in a short period of time, with the resulting The impact is not a good experience for the visually impaired.

The tension response curve during spring guidance is shown in Figure **12**. The horizontal coordinates indicate time and the vertical coordinates indicate the tension values. Given the horizontal abrupt pull at the end of the spring, that is, the guide robot applies a step pull of 5N-15N to the end of the rigid rod over a period of 2-15s. The horizontal tension applied at the end of the spring is shown as the colour curve in Figure **12**. The tension applied to the first end of the spring can be expressed as the synthesis of the gravitational force of the spring and the horizontal tension at the end. Data was collected using a tension sensor at the end of the guide robot and the force curve was plotted on an Origin software post-processor.

The force curve has an initial value of approximately 2.5 N due to the spring's own gravity and the limitations of the experimental conditions, and the purple curve does not follow the blue dashed line due to the limited length of the spring pull up due to the limitations of the experimental site. The non-linearity of the tension response curve is more pronounced when the tension F<8N. When F>8N, the non-linearity of the spring tension step response curve is significantly reduced. The experimental data curves show that the spring conducts force very slowly and the linearised green and purple response curves show that the tension rise time is greater than 15s and there is a very obvious hysteresis effect. The length of the spring being pulled up is also beyond the normal reasonable distance.

The tension response curve for the flexible cable guide is shown in Figure **13**. The horizontal coordinates represent time and the vertical coordinates represent the tension values. Given a sudden horizontal pull at the end of the flex cable, *i.e*. a step pull of 10N-35N is applied to the end of the flex cable by the guide robot over a period of 1-4s. The horizontal tension applied at the end of the flex cable is shown in the colour curve in Figure **13**. The tension applied to the first end of the cable can be expressed as a combination of the gravitational force of the cable and the horizontal tension at the end. Data was collected using a tension sensor at the end of the guide robot and the force curve was plotted on an Origin software post-processor.

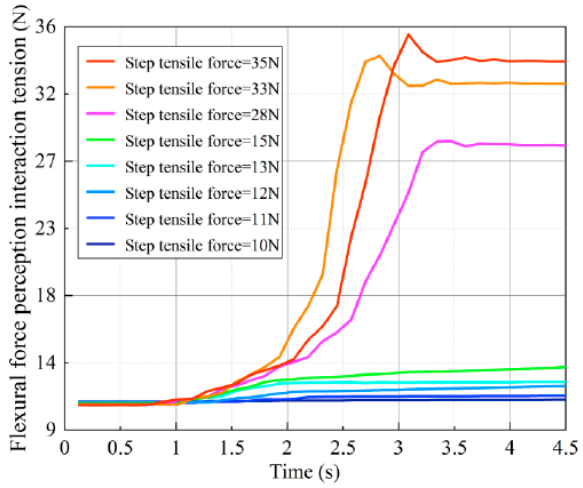

Figure 13: Step response curve for flexural force perception interaction tension.

Due to the gravity of the flexible cable and the limitations of the experimental conditions, the tension curve fluctuates around the peak and produces an initial value of about 11 N. When the tension F < 20 N, the step response curve of the tension does not change significantly. And when F>20N, there is an obvious non-linear upward process in the step response curve of the flexible cable pulling force. From the above experimental data curve, we can see that the transmission process of the flexible cable to the tension is relatively moderate, the tension rise time is about 1~2s on average, and the flexible cable is not as likely to be wirelessly stretched as the spring. The cable does not produce a large force impact on the human, which reduces the experience, but also allows the visually impaired to respond to the robot's guidance in a timely manner. There is some lag, but not so much that the visually impaired person loses their sense of purpose. It therefore meets the requirements for pace synergy between the visually impaired and the guide dog.

5. CONCLUSION

After the theoretical analysis and experimental verification of the force transmission effects of the three types of force perception interaction media, rigid rods, springs and flexible cables, their force transmission characteristics can be briefly summarised as follows.

1. rigid rods: rapid force transmission and low loss.

2. springs: force transmission with some fluctuation and hysteresis, the fluctuation and hysteresis effect being related to the stiffness and damping coefficients of the springs

3. Flexible ropes: the end tension is related to the relative distance between the two ends of the flexible ropes. Before the flex cable is stretched to its original length, the end tension is mainly influenced by its gravity; after the flex cable is stretched to its original length, its end tension is mainly influenced by its elasticity.

For the engineering application of flexure interaction, we would prefer that the force-aware interaction meets the natural fluidity requirements of the force-aware interaction process, *i.e*. we would like the interaction medium to be 'soft'. At the same time, we would like the force information to be extracted and analysed in order to better suit the movement of the blind, *i.e*. we would like the interaction medium to be 'hard'. By comparing the mechanical properties of these three interaction media, we have chosen a flexible cable as the force-aware interaction medium for a guide dog robot and have carried out theoretical research on the subject.

Since this paper has only done the preliminary fundamental research for the force interaction medium proposed in this paper, and still does not have the integrity analysis of the actual engineering landing, we plan to make a strong research demonstration on the reliability and error of the model and other aspects of the model in the further research in the future.

ACKNOWLEDGMENTS

Thanks are due to my lab colleagues for assistance with the experiments and to my mentor for valuable discussion.

DECLARATIONS CONFLICT OF INTEREST

The authors declare that they have no competing interests.

REFERENCES

[1] Zhu, J., *et al*. An Edge Computing Platform of Guide-dog Robot for Visually Impaired. in 2019 IEEE 14th International Symposium on Autonomous Decentralized System (ISADS). 2019. https://doi.org/10.1109/ISADS45777.2019.9155620

[2] Sveny, B., G. Kovacs, and Z.T. Kardkovacs, Blind guide - A virtual eye for guiding indoor and outdoor movement. IEEE, 2015. https://doi.org/10.1109/CogInfoCom.2014.7020476

[3] Mancini, A., E. Frontoni, and P. Zingaretti, Mechatronic System to Help Visually Impaired Users During Walking and Running. IEEE Transactions on Intelligent Transportation Systems, 2018. PP(2): p. 1-12. https://doi.org/10.1109/TITS.2017.2780621

[4] Katzschmann, R., B. Araki, and D. Rus, Safe Local Navigation for Visually Impaired Users with a Time-of-Flight and Haptic Feedback Device. IEEE Transactions on Neural Systems & Rehabilitation Engineering, 2018. PP(99): p. 1-1.

[5] Dong-Hyuk, *et al*., Tactile Navigation System using a Haptic Device. Journal of Institute of Control, Robotics and Systems, 2014. 20(8): p. 807-814. https://doi.org/10.5302/J.ICROS.2014.14.9039

[6] Wang, R.R., L.I. Xiao-Hong, and T. Chen, A Walking Assistant System for the Visually Impaired Based on Tactile Perception. Journal of Shanxi Datong University(Natural Science Edition), 2018.

[7] Mutiara, G.A., G.I. Hapsari, and R. Rijalul. Smart guide extension for blind cane. in International Conference on Information & Communication Technology. 2016. https://doi.org/10.1109/ICoICT.2016.7571896

[8] Guerreiro, J., *et al*. Cabot: Designing and evaluating an autonomous navigation robot for blind people. in 21st International ACM SIGACCESS Conference on Computers and Accessibility, ASSETS 2019, October 28, 2019 - October 30, 2019. 2019. Pittsburgh, PA, United states: Association for Computing Machinery. https://doi.org/10.1145/3308561.3353771

[9] Zeng, L., D. Bornschein, and G. Weber, Exploration and avoidance of surrounding obstacles for the visually impaired. ASSETS'12 - Proceedings of the 14th International ACM SIGACCESS Conference on Computers and Accessibility, 2012. https://doi.org/10.1145/2384916.2384936

[10] Mfj, A., *et al*., Assistive Locomotion Device with Haptic Feedback For Guiding Visually Impaired People. Medical Engineering & Physics, 2020.

[11] Zeng, L., *et al*. Hapticrein: Design and development of an interactive haptic rein for a guidance robot. in 16th International Conference on Computers Helping People with Special Needs, ICCHP 2018, July 11, 2018 - July 13, 2018. 2018. Linz, Austria: Springer Verlag.

[12] Kim, D.Y. and K.Y. Yi. A user-steered guide robot for the blind. in IEEE International Conference on Robotics & Biomimetics. 2009.

[13] Lacey, G. (1997). Evaluation of Robot Mobility Aid for the Elderly Blind.

[14] Xiao, A, Tong, W., Yang, L., Zeng, J., Li, Z., & Sreenath, K. (2021). Robotic guide dog: leading a human with leash-guided hybrid physical interaction. https://doi.org/10.1109/ICRA48506.2021.9561786

[15] Tognon, M., Alami, R., & Siciliano, B. (2020). Physical human-robot interaction with a tethered aerial vehicle: application to a force-based human guiding problem. https://doi.org/10.1109/TRO.2020.3038700

Received on 24-10-2023 Accepted on 22-11-2023 Published on 02-12-2023

DOI: https://doi.org/10.31875/2409-9694.2023.10.08

© 2023 Hong *et al.*; Licensee Zeal Press.
This is an open access article licensed under the terms of the Creative Commons Attribution Non-Commercial License (http://creativecommons.org/licenses/by-nc/3.0/), which permits unrestricted, non-commercial use, distribution and reproduction in any medium, provided the work is properly cited.